Tabular method of estimating nucleating steam flows

F. Bakhtar and R. A. Webb*

In the pressure range 0.04–1 bar the time necessary for steam to revert from a series of initial degrees of supercooling to thermodynamic equilibrium and the resulting fluid parameters have been tabulated. Application to practical flow conditions is discussed

Key words: *Steam + nucleation, fluid physics, steam turbines*

The importance of supersaturation in the separation of liquid phase from steam undergoing expansion has been recognised since the beginning of the century. The terms Wilson point and Wilson zone were introduced to describe the limiting conditions when the fluid first becomes wet. Traditionally, however, the procedures for calculating the behaviour of steam in the two-phase region are based on the use of steam tables which assume that the fluid remains in thermodynamic equilibrium throughout, becoming wet immediately on crossing the saturation line and totally disregard the detailed behaviour of the liquid phase. For any realistic treatment of the subject it is necessary to allow for the detailed behaviour of the liquid.

Nucleation theory has provided a better insight into the underlying physical phenomena and the combination of the results of this theory with the equations describing the one-dimensional flows of a compressible fluid are almost standard[1,2]. Extensions of the method to two- and three-dimensional flows are being developed[3,4] and their application to design problems is only a matter of time. Because of the complexity of the computations involved, there is a need for a simpler treatment so that an estimate can be made of the likely behaviour of the fluid without embarking on a prolonged calculation. The results presented in this paper were calculated towards this aim with the hope that they will prove of some value both to the specialists in the field and to the wider understanding of the subject.

Theoretical background

The Kelvin–Helmholtz equation relating the vapour pressure over a curved surface to its radius of curvature at low pressure is:

$$r^* = \frac{2\sigma}{\rho_L R T_G \ln [p/p_s(T_G)]} \tag{1}$$

where $p_s(T)$ is the saturation pressure corresponding to temperature T. For given vapour conditions, droplets with a radius of r^* will be in unstable equilibrium with the vapour. Larger droplets need a lower supersaturation for equilibrium and will grow under the prevailing conditions while smaller droplets will find the surrounding supercooling insufficient and tend to evaporate.

The existence of the critical radius is a barrier to the condensation of a pure vapour removed from contact with external surfaces. In order to condense the molecules must form a droplet of radius r^* which is against their natural tendency. The only route to the formation of super critical droplets is through the chance collisions within the body of the vapour. It will be seen from Eq (1) that r^* and $\ln p/p_s(T)$ are inversely related. Thus the lower the supersaturation, the larger the size of the critical droplets and the smaller the chance that they will be formed. For this reason, although an expanding vapour will begin to nucleate as soon as it has crossed the saturation line, the nucleation rate is initially extremely small and the vapour will supercool.

The rate of formation of critical clusters within the body of a scupercooled vapour was originally studied by Volmer and Weber[5], Frakas[6], Becker and Doring[7], Frenkel[8], Zeldovich[9] and has been subsequently refined, modified and reviewed by numerous investigators. It is beyond the scope of the present paper to review them. A lucid discussion of the derivation of the classical expression is given by McDonald[10] and a full and rigorous treatment of the subject is given by Dunning[11]. The expression for the nucleation rate as the number of droplets formed per unit volume and time as given by the classical theory is

$$J = q\left(\frac{2\sigma}{\pi m^3}\right)^{1/2} \frac{\rho_G}{\rho_L} \exp\left[-\frac{4\pi r^{*2}\sigma}{kT}\right] \tag{2}$$

where q, the condensation coefficient, is the fraction of molecular collisions which result in condensation.

The dominant term in Eq (2) is the exponential; substituting for r^* in terms of the supersaturation ratio, it will be seen that very small changes in the supersaturation of the fluid can influence the nucleation rate drastically.

The formation of droplets is part of the sequence which restores the vapour to equilibrium as, once the droplets form, they will interact with the

* Department of Mechanical Engineering, University of Birmingham, Edgbaston, Birmingham B15 2TT, UK
Received 7 September 1982 and accepted for publication in revised form on 11 August 1983

 0142-727X/83/040217-11$03.00

vapour and grow. The latent heat of condensing molecules is initially given up to the droplets then transferred to the vapour and eventually restores the system to equilibrium. In an expanding vapour, although the processes of droplet formation and growth begin as soon as the vapour has become supercooled, because of the great sensitivity of the nucleation rate to the supercooling of the fluid, the largest numbers of droplets are formed at the position of maximum supercooling. The distribution of the droplets has a peak corresponding with those formed at the Wilson point. Furthermore, the very assumption of supercooling indicates that the liquid formed within the fluid has been insufficient to affect the vapour temperature and the substantial release of latent heat, by definition, occurs after the Wilson point.

The experimental investigations of nucleation in flowing steam have, of necessity, been carried out in the diverging part of convergent–divergent nozzles, where the expansion is uniform. Consequently, the results of these experiments are usually correlated in terms of the rate of expansion[12]. This method is useful for predicting flows in which the expansion is uniform but in the majority of practical applications the rate of expansion varies considerably. In fact once the fluid has become supercooled, given sufficient time it will revert to thermodynamic equilibrium without further expansion.

Because of the prominence of the droplets formed at the Wilson point and the fact that in practical problems the variations in the rate of expansion are large, it is proposed in this paper to present some data on the reversion of steam when the rate of expansion is zero. For this purpose it is assumed that a given amount of supercooling is suddenly imposed on the vapour. Following this the time necessary for fluid to revert to thermodynamic equilibrium has been calculated. It is then proposed that for steam expanding from an initially dry state its behaviour be estimated from an assumption that it will supercool. Then at any particular strategic location the pressure and temperature of steam should be estimated. Following this, with the conditions as calculated a reference should be made to the tabulated data for the necessary reversion time. Then comparison between this reversion time and the time taken by the real fluid to traverse the region of interest will indicate whether the nucleation will be significant. It is accepted that such a procedure is no substitute for detailed numerical analysis; nevertheless it is claimed that this approach will provide a useful guide for estimating the overall behaviour of the fluid without elaborate computations. Although the calculations could have been carried out at constant volume, anticipating that such problems are more likely to arise in open systems, they have been performed at constant pressure.

Method of calculation

Condensing flows of steam can be taken as special cases of the compressible flows of the parent vapour phase in which the heat addition is the result of the phase change, which also affects its mass flow rate. To estimate the general behaviour of the system at low pressures, the earlier treatments regarded steam as a perfect gas and the standard equations of one-dimensional gas dynamics were employed. This approach has the disadvantage of disregarding the variations in the thermodynamic properties near and below the saturation line and is not suitable for comparing the paths of different expansions. For this purpose it is necessary to use thermodynamic properties which are mutually consistent. Such consistent properties can be calculated by adopting equations describing the saturation line, the specific heat at zero pressure and a suitable equation of state. Of these the first two present no problems and an examination of possible equations of state for describing properties of supercooled steam, showed the virial equation developed by Vukalovich to be most suitable[13]. However, for the case of steam at low and moderate pressures, as a compromise between accuracy and volume of algebra the equations can be truncated at the second virial term. The details of the necessary modifications of the governing equations have been given in the context of application to high pressure steam[14]. It has subsequently been found preferable to

Notation

h_{fg}	Enthalpy of evaporation
J	Nucleation rate
k	Boltzmann constant
m	Mass of a water molecule
Ma	Mach number
N	Number of droplets per unit mass
p	Pressure
q	Condensation coefficient
r	Radius of droplets
R	Gas constant
Δs	Increase in entropy of the fluid on reversion to equilibrium
t	Time
T	Temperature
$T_s(p)$	Saturation temperature corresponding to pressure p
ΔT	Degrees of supercooling, the difference between the saturation temperature corresponding to the local pressure and the fluid temperature
w	Wetness fraction
x	Distance along flow path
ρ	Density
σ	Surface tension

Subscripts

G	Vapour phase
L	Liquid phase

Superscript

*	Critical droplet or Wilson condition

include the higher virial terms at the higher pressures. With the availability of modern computers, even at low pressures the inclusion of the second virial coefficient is regarded as the minimum refinement necessary for obtaining adequate results.

The method used for these calculations is, therefore, based on this approach and has already been described in detail[14]. As described in this reference, apart from refinements necessitated by the introduction of the second virial coefficient, the nucleation rate was calculated by using the classical theory subject to the modifications proposed by Courtney[15] and by Kantrowitz[16]. The specific surface free energy of a small cluster was taken to be the same as that for a flat surface and the condensation coefficient taken as unity.

To use the above treatment for the present purposes, two further points of practical importance have had to be met:

1. The procedure available is applicable to flowing steam while the results sought require the fluid to remain at constant pressure. To meet this condition the calculations were carried out for flow in a frictionless duct of constant cross sectional area and the velocities adopted were sufficiently small to ensure that any increases in the velocity of the fluid resulting from the thermodynamic changes were negligibly small.
2. The duration of nucleation must be estimated correctly. The problem may be illustrated with reference to Fig 1 which shows some results relating to the early stages of nucleation in steam at 0.15 bar and initially 41 °C supercooled.† To observe their individual behaviour, the droplets formed during each incremental step of the calculation have been regarded as a distinct group and treated separately. The calculated nucleation rate is 1.13×10^{23} droplets per kilogramme of vapour per second and the incremental distance steps taken correspond with a time interval of 0.6864 μs. Considering the changes in the supercooling of the fluid first, it will be seen that despite the high nucleation rate, this parameter is not perceptibly affected in the initial stages because of the very small size of the nucleated droplets. The same tendency is also apparent from the variations in the critical droplet size (r^*) which is unaffected at the beginning but increases as the fluid becomes less supercooled. To investigate the behaviour of the droplets the variations of the radii of each individual group is plotted separately on the figure. Taking the graph marked group (1) which shows the growth of the droplets formed in the first 0.6864 μs of the flow as an example, it will be seen that the rate of growth of the droplets is initially small but rises rapidly as soon as they grow beyond the critical radius. The pattern is similar for the next 10 groups but a different behaviour is observed in the case of group 12. With the depletion of the supercooling these droplets become smaller than the critical size and in fact evaporate. Thus, with the step size adopted, the nucleation process can be assumed to be effec-

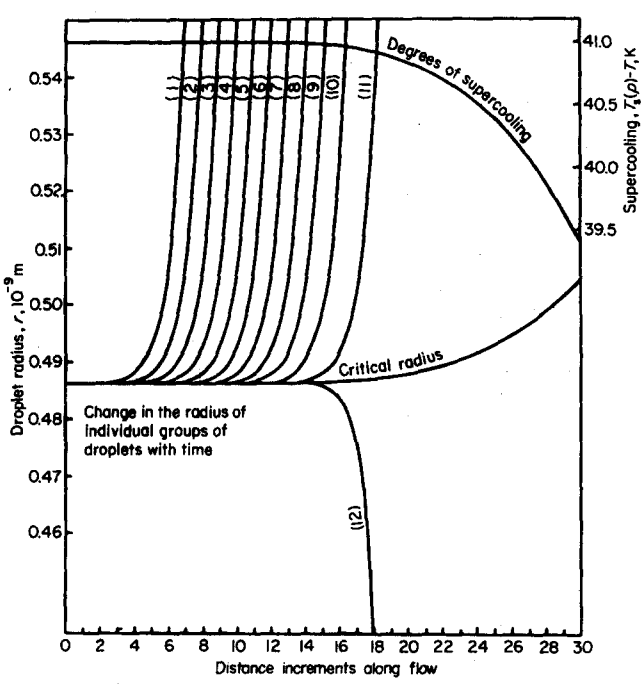

Fig 1 Development of the early stage of nucleation. The numbers on curves refer to specific groups

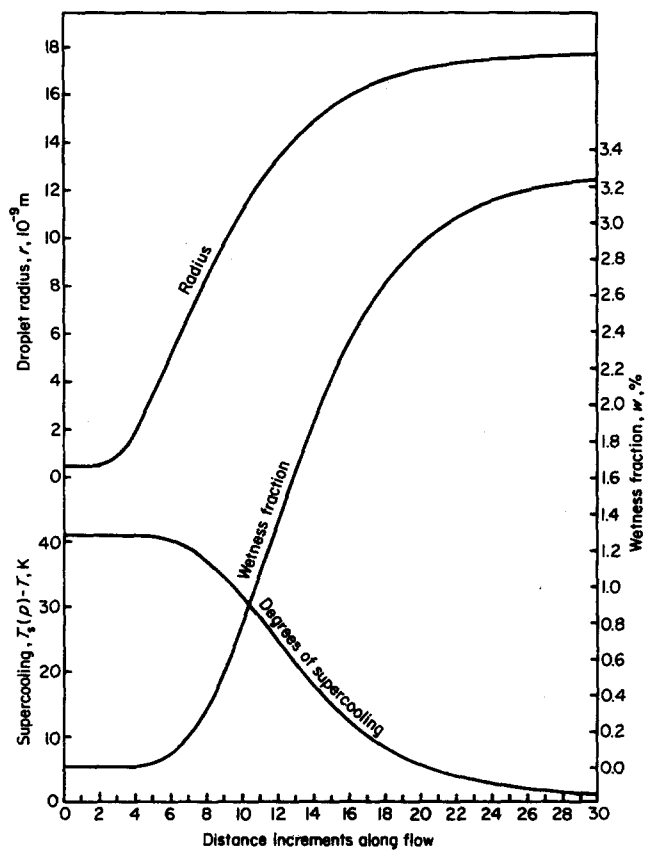

Fig 2 Changes in fluid properties during the return to equilibrium

† The degrees of supercooling are defined as the difference between the saturation temperature of the fluid corresponding to its local pressure and its temperature

tively over after the formation of group 11. By selecting a shorter step size the number of groups of droplets will increase but the number in each group will fall, increasing both the accuracy and the volume of algebra. In the calculation of the results presented, the step length was adjusted to keep the number of groups of droplets to approximately 10.

After the nucleation phase the groups of droplets were combined into a single population and described by mean properties with considerable savings in computation time. In the case of the example selected the changes in the relevant fluid properties with time after the nucleation phase are given in Fig 2. It will be seen that, as expected, after the nucleation stage the droplets grow rapidly at the beginning but with the depletion of supercooling the rate of growth slackens and becomes extremely slow as the fluid approaches thermodynamic equilibrium. But even at equilibrium some residual supercooling is enforced on the fluid by the curvature of the droplets.

Tabulated results

With the calculations thus completed the information extracted has been compiled in Table 1. The first two columns give the pressure and the initial degrees of supercooling respectively. For each given vapour condition, the corresponding values of the nucleation rate and the critical droplet radius are listed in the next two columns. To describe the transition to equilibrium, the time necessary for the fluid to attain wetness fractions of 0.01, 0.1 and 1.0% and the residual degrees of supercooling corresponding to each of these conditions are given.

In the case of the last stages of return to thermodynamic equilibrium, because of the presence of the irreversible heat transfer within the fluid, the calculations have been carried out far enough to ensure that the calculated entropy changes are accurate. The time taken by the flow to reach the point where the calculations have been truncated has been regarded as of little significance and is not tabulated. The data extracted relates to the residual degrees of supercooling, the wetness fraction, the radius of the resulting droplets on an rms basis and the entropy gained during the reversion process.

Thus for the example cited of steam at 0.15 bar and initially 41 K supercooled, the nucleation rate is 1.13×10^{23} droplets per kilogramme of vapour per second, and the critical droplets will have a radius of 4.86×10^{-10} m. The fluid will attain a wetness fraction of 0.01% in 12.9 μs by which time it will be 40.89 K supercooled. On reaching thermodynamic equilibrium the steam will be 3.287% wet containing droplets of mean radius 0.0199 μm which impose 0.94 K of supercooling on the surrounding vapour. The entropy gained by the fluid in returning to equilibrium is 15.42 J/(kg K). Further information may be obtained by simple deduction from these results. For example the thermodynamic loss incurred by the flow during reversion will be the product of the entropy gain and the local saturation temperature and the average size of the droplets at any other wetness fraction can be obtained by scaling from the equilibrium values.

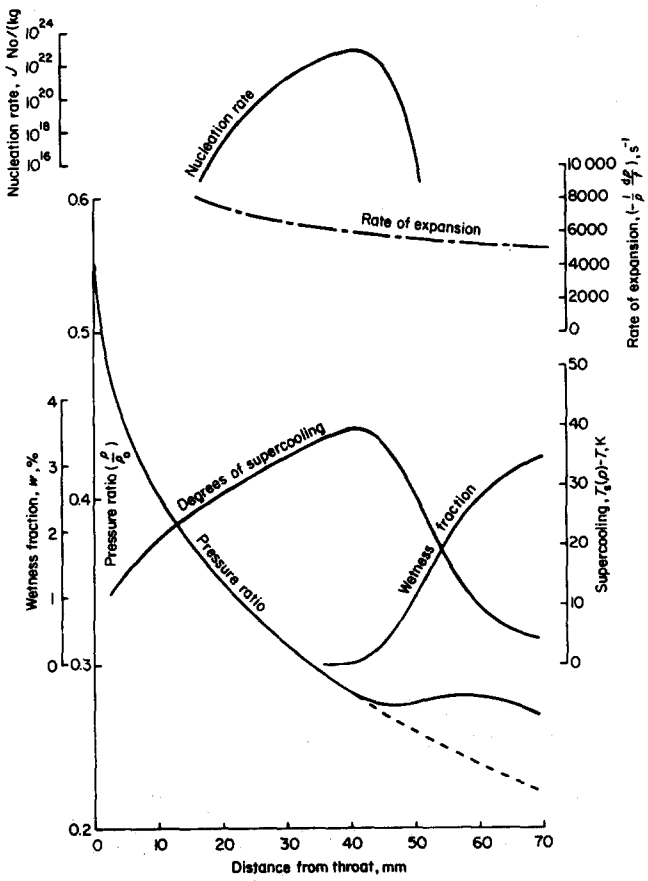

Fig 3 Typical example of changes in the fluid in the nucleation zone of a supersonic nozzle

Application of the tables

At low pressures and starting with dry saturated vapour, the critical heat drop does not supercool steam sufficiently to cause a high nucleation rate. Furthermore the release of the enthalpy of phase change retards the stream when the flow is supersonic while the converse is true for subsonic flows. For these reasons alone, subsonic and supersonic flows would have different characteristics in relation to nucleation and, in terms of the application of the tables, distinction should be drawn between them.

A typical case of the changes in a number of fluid properties in the nucleation zone in a supersonic flow is shown in Fig 3. The results are for the expansion of steam from a stagnation pressure of 1.034 bar in a frictionless nozzle having a throat width of 7.62 mm and an angle of divergence of 2°. The dotted line shows the axial pressure distribution when the stagnation temperature has been sufficiently high to maintain the steam in a dry stable state throughout. The full lines represent the axial distribution of a number of fluid properties when the stagnation temperature has been reduced to 411.1 K.

It will be seen that the maximum supercooling occurs 40.89 mm downstream of the throat. At this position the wetness formed within the flow is 0.066% which is insufficient to affect its temperature appreci-

ably and the wet and dry pressure distributions have not yet begun to diverge. Thus, up to this limiting condition the supercooled and superheated vapours have similar expansion indices. Making this assumption and neglecting the presence of the small quantity of water at the Wilson point, the maximum supercooling can be estimated by trial and error from the tabulated results but the arithmetic will be rather tedious.

Noting that the axial pressure distribution in nucleating flows shows a characteristic knee in the zone of rapid condensation, an easier method would be to use the extent of this zone and the local fluid

Table 1

				$w=0.01\%$		$w=0.1\%$		$w=1.0\%$		*Equilibrium*			
P, bar	ΔT, K	J, No/(kg s)	r^*, 10^{-10} m	t, μs	ΔT, K	t, μs	ΔT, K	t, μs	ΔT, K	ΔT, K	w, %	r, μm	ΔS, J/(kg K)
0.04	29	5.68×10^{15}	6.38	1961	28.86	3095	27.73	6766	16.16	0.022	2.244	0.743	9.35
	31	2.44×10^{17}	5.96	692	30.86	1129	29.73	2321	18.15	0.061	2.398	0.298	10.68
	33	6.28×10^{18}	5.59	319	32.86	544	31.74	1141	20.34	0.13	2.550	0.136	12.08
	35	9.20×10^{19}	5.27	164	34.86	272	33.74	536	22.38	0.25	2.699	0.0707	13.56
	37	8.63×10^{20}	4.98	99.5	36.85	158	35.74	294	24.43	0.45	2.846	0.0397	14.99
	39	5.66×10^{21}	4.72	63.1	38.85	97.9	37.75	174	26.50	0.74	2.988	0.0242	16.43
	41	2.78×10^{22}	4.49	42.8	40.88	59.7	39.76	97.7	28.62	1.13	3.127	0.0157	17.80
	43	1.07×10^{23}	4.28	33.2	42.88	42.9	41.78	69.2	30.72	1.57	3.265	0.0114	19.18
	45	3.41×10^{23}	4.08	25.1	44.89	33.4	43.80	51.5	32.86	2.11	3.400	0.00846	20.47
	47	9.17×10^{23}	3.91	20.6	46.89	27.0	45.82	40.6	34.99	2.64	3.536	0.00674	21.85
0.05	29	8.31×10^{15}	6.44	1518	28.86	2439	27.73	5353	16.24	0.028	2.258	0.710	9.14
	31	3.18×10^{17}	6.04	550	30.86	901	29.74	1840	18.24	0.061	2.413	0.289	10.43
	33	5.11×10^{18}	5.69	276	32.86	477	31.74	1006	20.42	0.12	2.567	0.150	11.81
	35	7.99×10^{19}	5.36	141	34.86	235	33.75	462	22.47	0.23	2.717	0.0762	13.23
	37	7.93×10^{20}	5.06	83.6	36.86	134	35.75	252	24.52	0.42	2.865	0.0430	14.68
	39	5.46×10^{21}	4.80	53.8	38.88	74.1	37.76	127	26.61	0.71	3.010	0.0255	16.06
	41	2.80×10^{22}	4.56	35.6	40.88	50.4	39.78	82.7	28.70	1.08	3.150	0.0166	17.42
	43	1.12×10^{23}	4.35	27.9	42.88	36.6	41.79	58.4	30.82	1.51	3.290	0.0120	18.82
	45	3.68×10^{23}	4.15	20.5	44.89	27.7	43.81	42.7	32.95	2.06	3.426	0.00875	20.04
	47	1.02×10^{24}	3.97	16.8	46.89	22.3	45.83	33.5	35.08	2.64	3.561	0.00682	21.31
0.06	29	1.13×10^{16}	6.49	1241	28.86	2002	27.74	4381	16.32	0.028	2.270	0.678	8.97
	31	4.33×10^{17}	6.09	449	30.86	736	29.74	1500	18.32	0.067	2.426	0.277	10.25
	33	8.70×10^{18}	5.73	216	32.86	370	31.75	769	20.50	0.13	2.580	0.136	11.60
	35	1.05×10^{20}	5.42	115	34.86	193	33.76	382	22.54	0.24	2.732	0.0750	12.97
	37	7.25×10^{20}	5.13	71.0	36.88	116	35.78	219	24.59	0.40	2.883	0.0454	14.40
	39	5.21×10^{21}	4.87	45.3	38.88	65.7	37.77	113	26.68	0.68	3.028	0.0268	15.79
	41	2.76×10^{22}	4.62	30.6	40.88	44.3	39.78	72.5	28.78	1.04	3.170	0.0174	17.11
	43	1.15×10^{23}	4.41	22.7	42.89	31.2	41.80	50.0	30.89	1.46	3.311	0.0125	18.46
	45	3.87×10^{23}	4.21	17.2	44.89	23.7	43.82	36.7	33.02	2.02	3.447	0.00900	19.68
	47	1.10×10^{24}	4.02	14.2	46.89	19.0	45.83	28.7	35.15	2.56	3.585	0.00709	21.02
0.07	29	1.48×10^{16}	6.53	1045	28.86	1683	27.75	3714	16.38	0.028	2.281	0.658	8.83
	31	5.62×10^{17}	6.13	378	30.87	678	29.76	1265	18.38	0.067	2.437	0.270	10.07
	33	1.13×10^{19}	5.77	177	32.86	304	31.76	628	20.56	0.14	2.595	0.132	11.13
	35	1.37×10^{20}	5.46	95.2	34.88	145	33.76	272	22.61	0.26	2.744	0.0703	12.76
	37	1.11×10^{21}	5.18	58.1	36.88	94.6	35.79	177	24.67	0.43	2.895	0.0421	14.15
	39	6.53×10^{21}	4.92	37.5	38.88	59.7	37.79	108	26.73	0.68	3.042	0.0269	15.55
	41	2.70×10^{22}	4.68	26,6	40.88	39.5	39.79	65.0	28.84	1.00	3.188	0.0182	16.88
	43	1.15×10^{23}	4.46	19.8	42.89	27.8	41.81	44.4	30.95	1.44	3.329	0.0127	18.17
	45	3.99×10^{23}	4.26	15.0	44.89	22.3	43.84	32.4	33.08	1.97	3.467	0.00924	19.41
	47	1.16×10^{24}	4.07	12.5	46.89	18.0	45.86	25.3	35.22	2.53	3.605	0.00720	20.71
0.08	29	1.88×10^{16}	6.57	899	28.86	1451	27.75	3193	16.44	0.028	2.291	0.631	8.70
	31	7.12×10^{17}	6.17	323	30.86	541	29.76	1085	18.45	0.072	2.448	0.258	9.92
	33	1.42×10^{19}	5.81	153	32.86	262	31.77	535	20.63	0.14	2.603	0.126	11.23
	35	1.72×10^{20}	5.49	82.3	34.88	138	33.79	267	22.67	0.27	2.757	0.0689	12.56
	37	1.40×10^{21}	5.21	47.8	36.88	76.0	35.77	133	24.74	0.47	2.906	0.0392	13.92
	39	8.22×10^{21}	4.95	32.2	38.88	51.3	37.80	93.0	26.80	0.70	3.056	0.0262	15.30
	41	3.72×10^{22}	4.72	22.1	40.88	34.7	39.82	54.3	28.91	1.04	3.201	0.0176	16.62
	43	1.15×10^{23}	4.50	17.8	42.89	25.0	41.81	40.3	31.00	1.38	3.347	0.0133	18.01
	45	4.06×10^{23}	4.30	13.2	44.89	18.7	43.83	29.1	33.14	1.92	3.485	0.00956	19.20
	47	1.20×10^{24}	4.11	10.8	46.89	14.8	45.85	22.5	35.28	2.47	3.625	0.00744	20.47
0.09	29	2.33×10^{16}	6.61	771	28.87	1288	27.76	2797	16.50	0.028	2.301	0.608	8.56
	31	8.81×10^{17}	6.20	281	30.87	479	29.76	952	18.50	0.072	2.458	0.249	9.80
	33	1.75×10^{19}	5.84	134	32.88	231	31.77	478	20.68	0.15	2.614	0.124	11.08
	35	2.10×10^{20}	5.52	71.9	34.88	120	33.79	232	22.73	0.28	2.768	0.0669	12.39
	37	1.71×10^{21}	5.23	41.8	36.88	66.7	35.78	116	24.80	0.48	2.918	0.0383	13.72
	39	1.01×10^{22}	4.98	28.3	38.88	45.0	37.81	81.3	26.86	0.73	3.067	0.0253	15.08
	41	4.57×10^{22}	4.75	19.1	40.89	28.9	39.80	47.7	28.97	1.06	3.212	0.0170	16.39
	43	1.67×10^{23}	4.54	14.7	42.89	21.0	41.81	33.8	31.08	1.48	3.356	0.0124	17.72
	45	4.10×10^{23}	4.34	11.7	44.89	16.9	43.84	26.4	33.19	1.86	3.504	0.00990	19.01
	47	1.24×10^{24}	4.15	9.56	46.89	14.1	45.87	20.2	35.34	2.46	3.642	0.00751	20.22

Table 1 (*cont*)

				w=0.01%		*w*=0.1%		*w*=1.0%		*Equilibrium*			
P, bar	Δ*T*, K	*J*, No/(kg s)	*r**, 10^{-10} m	*t*, μs	Δ*T*, K	*t*, μs	Δ*T*, K	*t*, μs	Δ*T*, K	Δ*T*, K	*w*, %	*r*, μm	Δ*S*, J/(kg K)
0.10	29	2.83×10^{16}	6.64	684	28.87	1137	27.77	2499	16.55	0.033	2.309	0.581	8.49
	31	1.06×10^{18}	6.23	249	30.87	445	29.77	1194	18.62	0.078	2.467	0.243	9.67
	33	2.11×10^{19}	5.87	120	32.88	204	31.78	416	20.73	0.16	2.623	0.121	10.96
	35	2.54×10^{20}	5.54	63.9	34.88	107	33.80	205	22.78	0.28	2.777	0.0649	12.26
	37	2.05×10^{21}	5.26	37.3	36.88	61.2	35.80	103	24.85	0.49	2.928	0.0376	13.56
	39	1.21×10^{22}	5.00	25.5	38.88	40.3	37.82	72.2	26.91	0.75	3.078	0.0246	14.87
	41	5.48×10^{22}	4.77	17.1	40.88	25.9	39.80	42.4	29.03	1.11	3.223	0.0166	16.15
	43	2.00×10^{23}	4.56	12.9	42.89	19.9	41.85	34.1	31.09	1.49	3.369	0.0124	17.49
	45	6.11×10^{23}	4.37	9.83	44.89	14.9	43.86	22.3	33.25	2.0	3.510	0.00926	18.73
	47	1.26×10^{24}	4.19	8.45	46.89	12.6	45.87	18.4	35.39	2.4	3.660	0.00771	20.04
0.15	29	6.44×10^{16}	6.76	428	28.87	815	27.79	1562	16.79	0.033	2.347	0.525	7.89
	31	2.34×10^{18}	6.34	154	30.88	274	29.81	535	18.92	0.083	2.507	0.220	9.03
	33	4.50×10^{19}	5.98	73.6	32.88	126	31.81	250	20.95	0.18	2.666	0.107	10.24
	35	5.25×10^{20}	5.65	39.3	34.88	65.8	33.82	125	23.01	0.33	2.822	0.0577	11.48
	37	4.24×10^{21}	5.36	23.6	36.89	38.5	35.83	70.8	25.08	0.54	2.975	0.0344	12.72
	39	2.49×10^{22}	5.10	16.6	38.87	24.2	37.83	42.6	27.17	0.73	3.131	0.0256	14.04
	41	1.13×10^{23}	4.86	12.9	40.89	19.3	39.86	33.4	29.23	0.94	3.287	0.0199	15.42
	43	4.11×10^{23}	4.65	10.2	42.86	13.8	41.85	21.8	31.38	1.45	3.431	0.0130	16.56
	45	1.24×10^{24}	4.45	8.00	44.89	11.3	43.89	18.0	33.45	1.90	3.579	0.00991	17.79
	47	3.29×10^{24}	4.27	6.28	46.90	8.74	45.89	13.1	35.61	2.35	3.728	0.00802	19.10
0.20	29	1.21×10^{17}	6.85	262	28.87	504	27.81	1313	17.03	0.033	2.377	0.588	7.72
	31	4.24×10^{18}	6.43	102	30.87	183	29.81	422	19.08	0.078	2.540	0.250	8.83
	33	8.09×10^{19}	6.05	54.0	32.88	95.1	31.83	206	21.12	0.16	2.701	0.121	10.00
	35	9.43×10^{20}	5.72	26.8	34.87	42.7	33.83	84.1	23.19	0.31	2.860	0.0624	11.20
	37	7.45×10^{21}	5.43	19.0	36.89	30.2	35.85	57.3	25.25	0.52	3.016	0.0364	12.38
	39	4.29×10^{22}	5.17	12.7	38.89	19.5	37.86	35.0	27.33	0.80	3.170	0.0238	13.60
	41	1.89×10^{23}	4.93	9.37	40.89	13.9	39.87	24.0	29.42	1.11	3.322	0.0166	14.80
	43	6.90×10^{23}	4.71	7.26	42.89	10.6	41.87	16.4	31.57	1.55	3.473	0.0123	16.01
	45	2.11×10^{24}	4.51	5.79	44.90	8.17	43.91	13.0	33.65	2.09	3.619	0.00910	17.09
	47	5.58×10^{24}	4.33	4.50	46.90	6.82	45.91	9.92	35.84	2.58	3.770	0.00737	18.28
0.25	29	2.03×10^{17}	6.92	217	28.88	382	27.83	1004	17.18	0.033	2.403	0.542	7.55
	31	7.02×10^{18}	6.49	76.8	30.88	138	29.83	317	19.22	0.083	2.567	0.230	8.65
	33	1.31×10^{20}	6.12	41.5	32.89	72.1	31.84	154	21.27	0.17	2.730	0.110	9.78
	35	1.48×10^{21}	5.78	23.2	34.89	38.1	33.86	75.4	23.33	0.33	2.891	0.0581	10.93
	37	1.16×10^{22}	5.49	14.7	36.89	23.3	35.86	44.1	25.40	0.56	3.048	0.0340	12.10
	39	6.67×10^{22}	5.22	9.86	38.89	13.2	37.86	22.8	27.52	0.88	3.203	0.0219	13.23
	41	2.97×10^{23}	4.98	7.07	40.89	9.45	39.88	15.5	29.64	1.28	3.354	0.0149	14.33
	43	1.07×10^{24}	4.76	5.45	42.90	7.55	41.90	11.7	31.76	1.75	3.505	0.0110	15.44
	45	3.16×10^{24}	4.56	4.19	44.90	5.57	43.92	8.55	33.91	2.32	3.653	0.00830	16.46
	47	8.36×10^{24}	4.38	3.39	46.90	4.58	45.94	6.88	36.05	2.83	3.805	0.00678	17.60
0.30	29	3.13×10^{17}	6.98	170	28.88	339	27.85	788	17.30	0.039	2.425	0.496	7.43
	31	1.06×10^{19}	6.55	67.3	30.89	122	29.85	246	19.35	0.094	2.592	0.209	8.48
	33	1.95×10^{20}	6.17	33.4	32.89	57.8	31.86	123	21.40	0.19	2.756	0.100	9.59
	35	2.21×10^{21}	5.83	18.4	34.89	30.2	33.87	59.0	23.46	0.36	2.918	0.0538	10.72
	37	1.71×10^{22}	5.53	11.5	36.89	18.1	35.88	33.6	25.54	0.60	3.077	0.0322	11.82
	39	9.69×10^{22}	5.27	7.89	38.89	10.7	37.88	18.1	27.66	0.95	3.231	0.0203	12.92
	41	4.25×10^{23}	5.02	5.55	40.89	7.38	39.90	12.1	29.78	1.39	3.383	0.0138	13.96
	43	1.53×10^{24}	4.80	4.33	42.90	6.17	41.91	9.57	31.90	1.82	3.537	0.0106	15.10
	45	4.63×10^{24}	4.60	3.42	44.90	5.66	43.93	8.10	34.06	2.42	3.686	0.00800	16.07
	47	1.21×10^{25}	4.42	2.70	46.91	3.71	45.96	5.52	36.23	3.08	3.834	0.00628	17.01
0.35	29	4.59×10^{17}	7.03	140	28.89	276	27.86	650	17.40	0.044	2.446	0.466	7.32
	31	1.53×10^{19}	6.60	55.3	30.89	99.6	29.86	200	19.46	0.10	2.614	0.194	8.36
	33	2.75×10^{20}	6.21	26.8	32.89	45.9	31.87	95.2	21.51	0.21	2.780	0.0937	9.44
	35	2.96×10^{21}	5.88	15.3	34.89	25.0	33.88	48.6	23.58	0.38	2.943	0.0511	10.55
	37	2.37×10^{22}	5.57	9.60	36.89	15.1	35.89	27.8	25.66	0.65	3.102	0.0298	11.61
	39	1.34×10^{23}	5.30	6.57	38.90	9.01	37.89	15.2	27.79	0.99	3.259	0.0195	12.70
	41	5.87×10^{23}	5.06	4.59	40.90	6.15	39.92	10.0	29.92	1.44	3.411	0.0131	13.67
	43	2.07×10^{24}	4.84	3.62	42.90	5.18	41.93	7.89	32.07	1.99	3.564	0.00977	14.68
	45	6.26×10^{24}	4.64	2.86	44.90	4.09	43.97	6.50	34.13	2.56	3.716	0.00758	15.68
	47	1.64×10^{25}	4.45	2.24	46.91	3.19	46.00	4.70	36.37	3.18	3.867	0.00612	16.64

Table 1 (*cont*)

				w=0.01%		*w*=0.1%		*w*=1.0%		*Equilibrium*			
P, bar	Δ*T*, K	*J*, No/(kg s)	*r**, 10^{-10} m	*t*, μs	Δ*T*, K	*t*, μs	Δ*T*, K	*t*, μs	Δ*T*, K	Δ*T*, K	*w*, %	*r*, μm	Δ*S*, J/(kg K)
0.40	29	6.41×10^{17}	7.07	117	28.89	230	27.87	546	17.47	0.044	2.466	0.439	7.15
	31	2.11×10^{19}	6.64	46.6	30.89	83.6	29.87	191	19.56	0.11	2.635	0.183	8.17
	33	3.76×10^{20}	6.25	22.7	32.89	38.7	31.88	79.7	21.62	0.22	2.802	0.0887	9.23
	35	4.17×10^{21}	5.91	12.9	34.89	21.0	33.89	40.5	23.69	0.40	2.966	0.0484	10.32
	37	3.15×10^{22}	5.61	8.23	36.89	12.8	35.90	23.4	25.77	0.67	3.127	0.0289	11.38
	39	1.77×10^{23}	5.34	5.44	38.89	7.42	37.91	12.5	27.91	1.06	3.283	0.0184	12.40
	41	7.74×10^{23}	5.09	3.90	40.90	5.25	39.93	8.50	30.04	1.50	3.437	0.0126	13.36
	43	2.76×10^{24}	4.87	3.08	42.90	5.12	41.96	7.46	32.19	2.03	3.594	0.00961	14.36
	45	8.27×10^{24}	4.67	2.35	44.90	3.26	43.98	4.93	34 35	2.68	3.744	0.00729	15.25
	47	2.13×10^{25}	4.48	1.90	46.90	2.81	46.00	4.11	36.52	3.29	3.899	0.00593	16.21
0.45	29	8.66×10^{17}	7.12	101	28.89	195	27.88	462	17.57	0.056	2.483	0.410	7.07
	31	2.81×10^{19}	6.68	40.1	30.89	71.9	29.89	165	19.66	0.11	2.654	0.175	8.09
	33	4.96×10^{20}	6.29	19.7	32.89	33.4	31.89	68.9	21.71	0.23	2.823	0.0852	9.11
	35	5.46×10^{21}	5.95	11.1	34.89	18.0	33.90	34.6	23.79	0.43	2.987	0.0458	10.19
	37	4.11×10^{22}	5.64	7.07	36.89	11.1	35.92	20.1	25.87	0.71	3.149	0.0276	11.20
	39	2.27×10^{23}	5.37	4.72	38.90	6.47	37.93	10.8	28.02	1.11	3.307	0.0177	12.20
	41	9.90×10^{23}	5.12	3.38	40.90	4.58	39.95	7.36	30.16	1.61	3.461	0.0121	13.13
	43	3.51×10^{24}	4.90	2.58	42.90	3.51	41.97	5.46	32.31	2.17	3.616	0.00902	14.08
	45	1.05×10^{25}	4.69	2.03	44.91	2.89	43.99	4.35	34.47	2.76	3.771	0.00709	14.99
	47	2.73×10^{25}	4.51	1.64	46.91	2.47	46.02	3.58	36.66	3.52	3.921	0.00557	15.78
0.50	29	1.18×10^{18}	7.15	87	28.89	167	27.89	392	17.67	0.05	2.501	0.382	6.99
	31	3.70×10^{19}	6.71	34.3	30.89	60.9	29.89	121	19.75	0.12	2.672	0.160	7.98
	33	6.37×10^{20}	6.32	17.1	32.89	29.1	31.90	59.6	21.97	0.24	2.841	0.0812	9.04
	35	6.95×10^{21}	5.98	9.75	34.89	13.9	33.91	25.8	23.90	0.45	3.007	0.0437	10.06
	37	5.20×10^{22}	5.67	6.23	36.90	9.71	35.93	17.6	25.97	0.73	3.171	0.0266	11.07
	39	2.88×10^{23}	5.40	4.14	38.90	6.31	37.94	11.0	28.08	1.14	3.330	0.0172	12.06
	41	1.24×10^{24}	5.15	2.96	40.90	4.04	39.96	6.45	30.26	1.67	3.483	0.0116	12.95
	43	4.37×10^{24}	4.92	2.26	42.91	3.12	41.98	4.84	32.42	2.23	3.640	0.00878	13.85
	45	1.31×10^{25}	4.72	1.78	44.91	2.57	44.01	3.83	34.60	2.91	3.793	0.00675	14.69
	47	3.39×10^{25}	4.53	1.44	46.92	2.25	46.06	3.23	36.78	3.68	3.944	0.00534	15.48
0.60	29	2.01×10^{18}	7.21	68	28.89	129	27.90	301	17.84	0.056	2.532	0.345	6.88
	31	6.12×10^{19}	6.77	26.8	30.89	47.3	29.91	93.9	19.91	0.13	2.706	0.147	7.85
	33	1.03×10^{21}	6.38	13.6	32.90	22.8	31.92	46.4	21.96	0.27	2.877	0.0744	8.87
	35	1.09×10^{22}	6.03	7.73	34.90	12.5	33.93	23.7	24.05	0.48	3.045	0.0405	9.86
	37	7.85×10^{22}	5.72	4.89	36.90	7.61	35.95	13.7	26.14	0.81	3.209	0.0242	10.83
	39	4.31×10^{23}	5.45	3.32	38.90	4.64	37.96	7.61	28.30	1.23	3.370	0.0160	11.78
	41	1.85×10^{24}	5.19	2.36	40.90	3.25	39.98	5.16	30.45	1.79	3.526	0.0110	12.65
	43	6.49×10^{24}	4.97	1.81	42.91	2.53	42.00	3.87	32.63	2.44	3.682	0.00807	13.43
	45	1.92×10^{25}	4.76	1.42	44.91	2.13	44.03	3.15	34.81	3.09	3.838	0.00631	14.24
	47	4.92×10^{25}	4.57	1.17	46.92	1.69	46.06	2.47	37.02	3.92	3.992	0.00500	14.90
0.70	27	5.05×10^{18}	7.77	180	26.89	459	25.91	1152	15.93	0.028	2.384	0.830	5.82
	29	3.20×10^{19}	7.26	54.8	28.89	103	27.92	236	18.00	0.067	2.561	0.309	6.74
	31	9.42×10^{19}	6.82	21.6	30.90	38.2	29.93	83.5	20.05	0.14	2.736	0.135	7.71
	33	1.55×10^{21}	6.42	11.0	32.90	18.6	31.94	38.2	22.11	0.29	2.909	0.0681	8.67
	35	1.61×10^{22}	6.08	6.24	34.90	10.1	33.95	19.1	24.20	0.52	3.079	0.0380	9.65
	37	1.16×10^{23}	5.77	3.90	36.90	6.11	35.96	10.9	26.30	0.86	3.245	0.0228	10.58
	39	6.24×10^{23}	5.49	2.75	38.91	4.15	37.98	7.10	28.42	1.31	3.407	0.0151	11.51
	41	2.59×10^{24}	5.24	1.94	40.91	2.90	40.00	4.84	30.56	1.87	3.566	0.0105	12.33
	43	9.05×10^{24}	5.01	1.49	42.91	2.13	42.03	3.24	32.80	2.55	3.721	0.00767	13.09
	45	2.67×10^{25}	4.80	1.17	44.92	1.71	44.05	2.71	34.88	3.17	3.884	0.00616	13.90
0.80	27	7.83×10^{18}	7.82	146	26.89	337	25.92	917	16.05	0.028	2.408	0.748	5.77
	29	4.82×10^{19}	7.31	45.8	28.89	84.8	27.93	231	18.11	0.072	2.587	0.284	6.66
	31	1.39×10^{20}	6.86	17.9	30.89	31.7	29.93	69.3	20.17	0.16	2.764	0.127	7.60
	33	2.24×10^{21}	6.46	9.29	32.90	15.4	31.95	30.8	22.24	0.31	2.939	0.0634	8.57
	35	2.28×10^{22}	6.11	5.19	34.90	8.37	33.96	15.7	24.33	0.56	3.110	0.0356	9.53
	37	1.62×10^{23}	5.80	3.28	36.90	5.13	35.98	9.14	26.44	0.92	3.278	0.0215	10.43
	39	8.61×10^{23}	5.52	2.22	38.90	3.16	37.99	5.10	28.62	1.42	3.440	0.0139	11.26
	41	3.60×10^{24}	5.27	1.64	40.91	2.44	40.02	4.06	30.71	1.96	3.603	0.00998	12.07
	43	1.24×10^{25}	5.04	1.25	42.91	1.87	42.04	2.82	32.96	2.63	3.762	0.00744	12.82
	45	3.55×10^{25}	4.83	0.991	44.92	1.45	44.07	2.30	35.04	3.46	3.914	0.00585	13.54

Table 1 (*cont*)

				w=0.01%		*w*=0.1%		*w*=1.0%		*Equilibrium*			
P, bar	Δ*T*, K	*J*, No/(kg s)	*r**, 10^{-10} m	*t*, μs	Δ*T*, K	*t*, μs	Δ*T*, K	*t*, μs	Δ*T*, K	Δ*T*, K	*w*, %	*r*, μm	Δ*S*, J/(kg K)
0.90	27	1.17×10^{17}	7.87	122	26.89	271	25.93	760	16.17	0.028	2.431	0.690	5.71
	29	7.00×10^{18}	7.35	38.2	28.90	71.4	27.94	194	18.22	0.072	2.612	0.271	6.61
	31	1.98×10^{20}	6.90	15.1	30.89	26.6	29.95	57.4	20.29	0.17	2.791	0.118	7.52
	33	3.12×10^{21}	6.50	7.6	32.90	12.8	31.96	25.2	22.37	0.33	2.967	0.0590	8.46
	35	3.14×10^{22}	6.15	4.45	34.90	7.11	33.97	13.2	24.46	0.59	3.140	0.0334	9.39
	37	2.18×10^{23}	5.84	2.82	36.90	4.40	35.99	7.81	26.57	0.98	3.308	0.0202	10.27
	39	1.15×10^{24}	5.55	1.91	38.90	2.71	38.01	4.38	28.75	1.45	3.473	0.0134	11.11
	41	4.78×10^{24}	5.30	1.36	40.91	2.05	40.03	3.09	30.92	2.11	3.632	0.00925	11.84
	43	1.63×10^{25}	5.07	1.02	42.91	1.53	42.06	2.22	33.12	2.93	3.783	0.00662	12.51
	45	4.73×10^{25}	4.86	0.793	44.92	1.19	44.09	1.73	35.34	3.77	3.940	0.00539	13.13
1.00	27	1.73×10^{17}	7.91	102	26.89	221	25.94	627	16.28	0.033	2.453	0.632	5.62
	29	9.96×10^{18}	7.39	32.9	28.89	60.4	27.95	155	18.33	0.083	2.635	0.244	6.50
	31	2.72×10^{20}	6.93	13.0	30.90	22.7	29.96	48.5	20.40	0.18	2.816	0.110	7.43
	33	4.22×10^{21}	6.53	6.52	32.90	10.9	31.97	21.4	22.48	0.36	2.993	0.0555	8.34
	35	4.19×10^{22}	6.18	3.88	34.90	6.18	33.98	11.4	24.58	0.63	3.167	0.0314	9.26
	37	2.90×10^{23}	5.87	2.37	36.90	3.73	36.00	6.61	26.69	1.03	3.337	0.0192	10.11
	39	1.51×10^{24}	5.58	1.66	38.90	2.53	38.02	4.32	28.85	1.51	3.504	0.0129	10.93
	41	6.16×10^{24}	5.33	1.39	40.91	1.83	40.04	2.88	31.01	1.91	3.679	0.0102	11.83
	43	2.09×10^{25}	5.10	1.06	42.92	1.47	42.07	2.21	33.20	2.67	3.834	0.00762	12.58
	45	6.04×10^{25}	4.89	0.887	44.92	1.22	44.13	1.77	35.41	3.44	3.996	0.00592	13.23

velocity to estimate the time taken by the flow to achieve a wetness fraction of 1%. This information can then be used for estimating the limiting supersaturation from the tables. However, condensation of steam in supersonic nozzles has been studied extensively in the literature and a substantial amount of data showing the extent of the condensation zone is already available.

The computer program developed at Birmingham University has already been used for comparison with a representative selection of these results and the agreement obtained has been satisfactory[17]. Using the program, the time necessary to achieve a wetness fraction of 1% in a series of frictionless ducts has been estimated. These are plotted as a function of the rate of expansion in Fig 4 as lines of constant Wilson point pressure to aid this calculation. With the Wilson point approximately determined, additional information regarding transition to equilibrium can be obtained by further reference to the tables. In the calculation of the results plotted in Fig 4 the values of the time have been selected to match the resulting droplet sizes and give limiting degrees of supercooling which are slightly lower than those obtained from direct calculations. An example of the use of the tables adopting this approach is given in Appendix 1.

The investigations of condensation in supersonic nozzles, however, represent only one aspect of condensing flows. It can easily be verified that unless the steam is already supercooled at inlet to a nozzle, expansion in the subsonic range does not supercool it sufficiently to cause rapid condensation. For this reason experimental observations of nucleation in subsonic flows are scarce. The few cases which have been examined are idealisations of flow in turbines[18,19]. The fluid can cross the saturation line at any point in turbine blading and consequently be supercooled at entry to the succeeding row. Taking the flow over the turbine stages shown diagrammatically in Fig 5 as an example, the main pressure drops occur over the blades, with little expansion occurring between the rows. Although in simple representations of equilibrium flows in turbines the gaps between the blade rows are regarded as of little importance, in the case of non-equilibrium flows, they have considerable significance as they can provide time for the fluid to recover thermodynamic equilibrium. Furthermore, because of the nature of compressible flows, the expansion in a subsonic nozzle is not uniform and a much higher proportion of the heat drop occurs in the high velocity proportion of the passage. Thus when estimating the flow over any given blade row, if the fluid is not already wet at inlet, it would be a reasonable approximation to assume that it will continue in the supercooled state until it reaches the end of the row. Once again the resulting degrees of supercooling are calculated and, with reference to Table 1, the time necessary for the reversion of the flow evaluated. If the time taken by the fluid to traverse the next gap is much smaller than this value the flow will again continue in a supercooled state over the

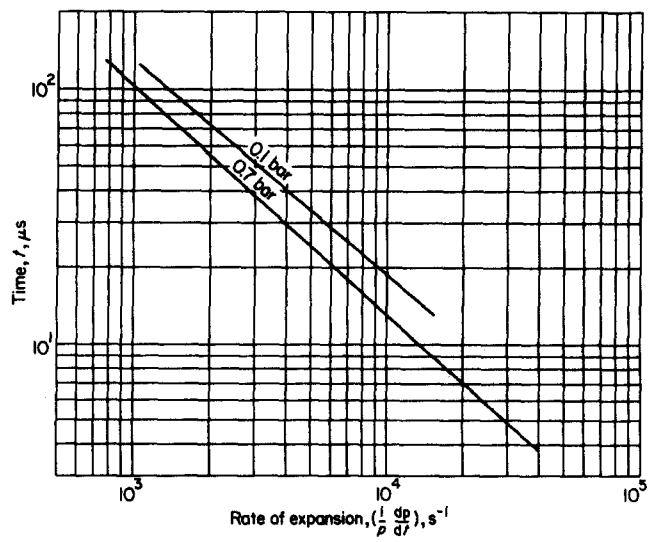

Fig 4 Variations in the time necessary for the formation of 1% wetness within steam with the rate of expansion in supersonic nozzles

Table 2

Location	x, cm	p, bar	Ma	ΔT, K	J, No/(kgs)	r, μm	w, %
Stator 1							
Inlet	0.0	0.375	0.17	—	—	—	—
Throat	4.32	0.250	0.78	20.7	5.8×10^{5}	—	—
End of blade	5.79	0.248	0.76	18.7	2.5	—	—
End of gap	8.33	0.198	0.92	26.6	5.2×10^{14}	—	—
Rotor 1							
Throat	1.42	0.145	0.73	41.7	1.8×10^{23}	0.0007	—
	1.88	0.139	0.76	40.1	5.6×10^{22}	0.0067	0.26
End of blade	2.18	0.124	0.85	33.3	5.0×10^{19}	0.011	1.25
	2.79	0.122	0.37	2.3	—	0.016	3.76
End of gap	7.29	0.122	0.26	1.1	—	0.016	3.57

next row of blades until finally the time necessary to revert to equilibrium is found to be less than is necessary to traverse the gap. Thus, the fluid can be assumed to reach its limiting condition in the throat region preceding this gap and the liquid terms obtained from Table 1. It is important, however, that any frictional reheat present within the flow be distributed realistically. If for the purposes of example the flow illustrated in Fig 5 can be assumed to revert after the throat region of the second row of stationary blades (point B in the figure), the expansion from A to B may be more efficient than that between A and C. The process is illustrated on the enthalpy–entropy diagram in Fig 6. When dealing with dry flows it is customary to draw the process path as a smooth curve connecting points A and C. In fact the losses occurring within the flow are not experienced by the fluid uniformly and the process path may be better represented by the line ABC and the supercooling achieved at B will be higher than that at C. A particular advantage of the tables is that once the overall fluid behaviour is established, it will allow the effects of small variations in the flow to be determined quickly.

The procedure may be illustrated by application to the expansion through the model turbine described by Bakhtar and Heaton[19]. In this investigation one-dimensional equivalents were constructed for the expansion through the machine. Table 2 is an extract from Table 1 of Ref 19 and gives the variations of a number of important fluid parameters as a function of the distance along the flow path and has been carried out for the mean overall conditions of the machine. The flow path over each blade row is divided into two sections, blade inlet to throat and throat to the end of the blade. Because of the geometrical configuration of this turbine and the loss model adopted, the main pressure drops over the blade rows are expected to occur between the inlets and throats of the blades. A substantial amount of the aerodynamic losses are introduced into the flow in the gaps between the blade rows. Because of the high velocity of the flow in the gap following the stator the introduction of the losses has caused a pressure drop over this section and some acceleration of the flow. The acceleration of the flow in the rotor between the throat and the end of the blade is a consequence of the addition of latent heat to the compressible stream. It will be seen that the fluid crosses the saturation line in the stator blade and the reversion process

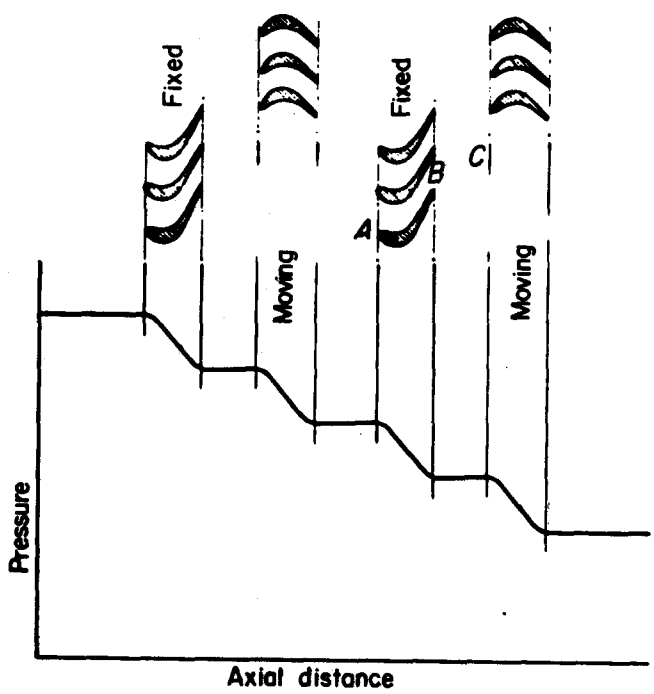

Fig 5 Flow in turbine stages

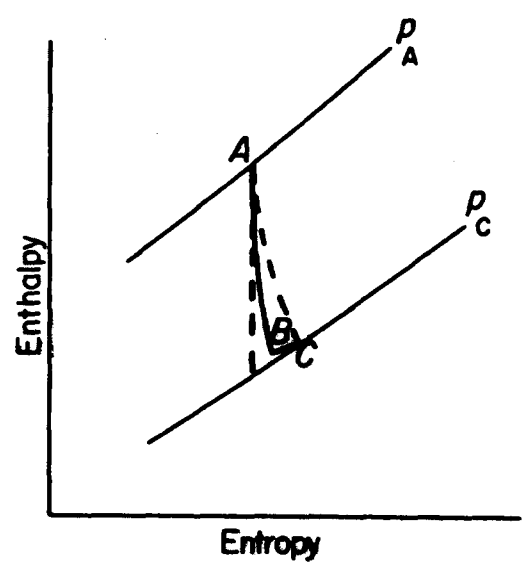

Fig 6 Process path for flow over a typical blade row

is completed by the end of the rotor gap. Variations in the rate of expansion and the nucleation rate along the flow path are plotted in Fig 7 and may be compared with the similar results for the nozzle flow in Fig 3.

With reference to the results in Table 2, the nucleation rates at the throat section of the stator and end of the stator gap are too small to be noticeable and the fluid enters the rotor 26.6 K supercooled. According to the procedure recommended for the use of Table 1 it should now be assumed that the flow expands between the inlet and the throat of the rotor blades in a supercooled state. Without the availability of the data used in the actual solutions it would now be necessary to estimate the efficiency of the expansion in this section of the blade and by estimating the isentropic enthalpy drop for supercooled steam over the particular pressure drop, calculate the steam temperature at the throat section. It will be seen from the results of the full calculations presented in Table 2 that the wetness formed within the flow is less than 0.005%. Thus the calculated temperature in the full solutions will not have been affected perceptibly by the release of the latent-heat due to the condensation of the liquid which has been formed. Consequently the results of the full solutions can be adopted for the purposes of using the tabular method. Thus the fluid attains 41.7 K of supercooling at the throat. Reference to the tables gives for this starting condition a time of 30.3 μs for the fluid to form 1% wetness and a droplet radius of 0.0177 μm at 3.57% moisture. The time taken by the fluid to travel from the rotor throat to the end of the rotor gap from the known velocities and distances is 377.9 μs, which is ample compared with the necessary time. Thus the flow will revert to equilibrium soon after the rotor throat. The estimated mean droplet radius at 3.57% moisture obtained in the full calculations is 0.016 μm.

In the case of expansion of wet steam, if the droplet size is known an estimate of the degrees of supercooling caused by the expansion can be made by first estimating the rate of condensation required by the flow. This can be done by estimating the necessary change in wetness fraction over the given pressure drop and the time available, to achieve it. From this estimate the necessary rate of growth of the droplets is calculated. In order to achieve this growth rate the latent heat of condensation given up to the droplets by the condensing molecules will have to be transferred back to the vapour. The necessary temperature difference between the droplets and the vapour $(T_L - T_G)$ to maintain this flow of heat can then be estimated. Finally the difference between the saturation temperature corresponding to the local pressure and the droplet temperature $T_s(p) - T_L$ can be estimated from the relationship:

$$T_s(p) - T_L = \frac{2\sigma T_s(p)}{h_{fg}\rho_L r} \tag{3}$$

which results from the combination of Kelvin–Helmholtz and Clausius–Clapeyron equations. The local degrees of supercooling attained by the flow is the sum of these two terms and reference to the tables will readily establish whether or not it will lead to significant nucleation.

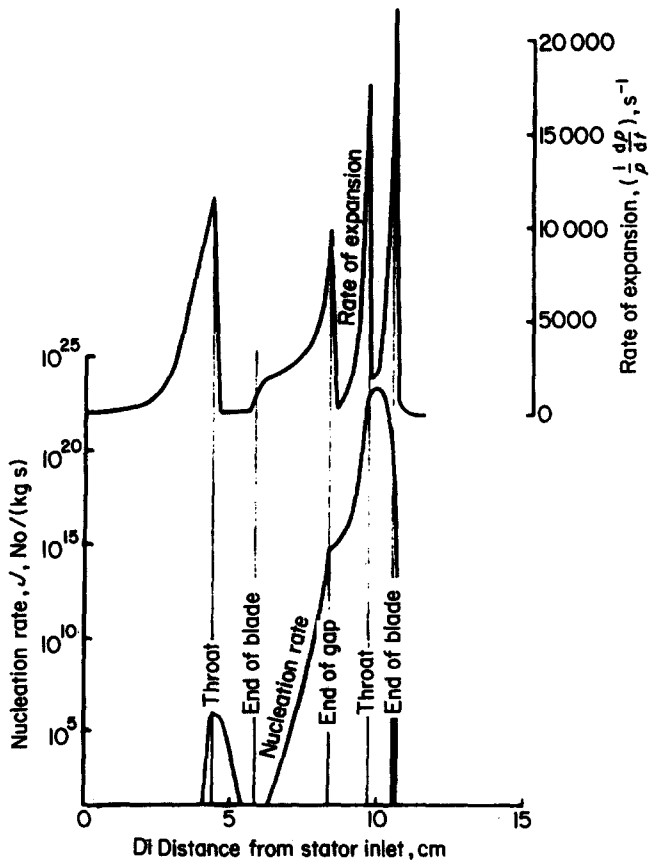

Fig 7 Variations of rate of expansion and nucleation rate in a typical turbine stage

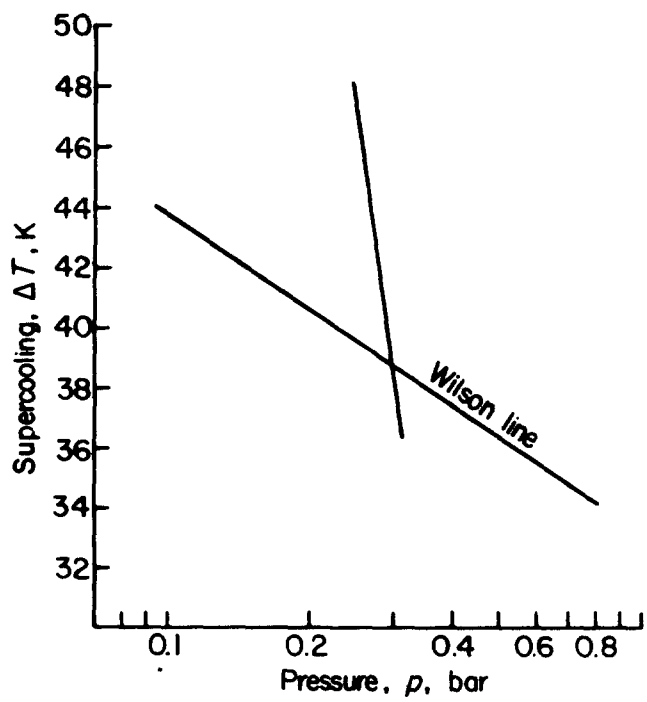

Fig 8 Graphical determination of the Wilson point

Conclusion

The tables meet the basic objective of providing a means of estimating the behaviour of nucleating steam without elaborate calculations. In the sense that the basic theoretical treatment has experimental support, the tabulated results are accurate but the quality of the results deduced from them depend on how well the detailed conditions of the flow are estimated. Nevertheless, within the aim of forming a ready appreciation of the likely behaviour of the flow, this is no hardship and experience will give better results.

Acknowledgements

The calculation of a simpler version of the above tables was originally started with assistance from Dr Chatwin and Mr W. M. Ip. The authors also acknowledge help from Mr M. Bessadi in the calculation of the results which have been presented.

Appendix 1 Numerical example on the use of tables

The procedure may be illustrated by considering the expansion of steam from stagnation conditions of 1.034 bar and 411.1 K in a frictionless convergent–divergent nozzle of constant depth with a throat width of 7.62 mm and total angle of divergence of 2°.

These conditions are the same as those considered in Fig 3. To use the recommended procedure it is first necessary to establish the rate of expansion for the nozzle which can be estimated from a dry expansion. In the present case, disallowing the formation of water the rate of expansion is plotted as a chain dotted line in Fig 3, from which the appropriate $\dot{p}$ can be read as $-5900\,s^{-1}$. Reference to Fig 4 gives 21 μs and 29.5 μs as the times taken by the fluid to form 1% wetness at 0.7 bar and 0.1 bar respectively. Using these values, reference to Table 1 gives the corresponding values of limiting degrees of supercooling at 0.7 and 0.1 bar as 34.8 and 43.78 K respectively. The simplest method of interpolation between these pressures is to plot these conditions as a straight line on semi-logarithmic paper (Fig 8) to produce an effective Wilson line.

To determine where the fluid crosses this condition it is only necessary to calculate the degrees of supercooling achieved by the fluid in frozen expansion from the given stagnation conditions. Adopting an isentropic index of 1.323 for the conditions of the problem, the calculated results for this case are given in Table 3.

Table 3

p, p_0	p, bar	$T_s(p)$, K	T/T_0	T, K	$T_s(p)-T$, K
0.30	0.3102	343.0	0.7453	306.4	36.6
0.28	0.2895	341.4	0.7329	301.3	40.1
0.26	0.2688	339.8	0.7197	295.9	43.9
0.24	0.2482	338.0	0.7058	290.2	47.8

These results are also plotted in Fig 8 and intersect the Wilson line at $p^*=0.3$ bar and $\Delta T^*=38.8$ K. Finally a check is made that the original rate of expansion was correctly chosen. Thus $p^*/p_0=0.29$ and reference to Fig 3 gives the expansion rate at this pressure ratio to be $6000\,s^{-1}$ which agrees with the original estimate reasonably well. Further reference to Table 1 gives the resulting droplet radii to be 0.0215 μm at a wetness fraction of 3.216%. These may be compared with the results of exact calculations which give a Wilson point pressure of 0.29 bar, the limiting degrees of supercooling as 39.34 K and the resulting droplet radii at similar wetness fraction as 0.02344 μm.

References

1. **Wegener P. P.** Gas dynamics of expansion flows with condensation and homogeneous nucleation of water vapour. *Gas Dynamics Vol. 1. Pt. 1., ed. P. P. Wegener, Marcel Dekker, NY 1969*
2. **Moore M. J. and Sieverding C. H.** Two phase steam flow in turbines and separators. *Hemisphere Publishing 1976*
3. **Bakhtar F. and Mohammadi Tochai M. T.** An investigation of two-dimensional flows of nucleating and wet steam by the time-marching method. *Int. J. Heat and Fluid Flow, 1980,* **2** *(1)*
4. **Yeoh C. C. and Young J. B.** Non-equilibrium streamline curvature throughflow calculations in wet steam turbines. *Proc. ASME, J. Engineering for Power, April 1982, 489–496*
5. **Volmer M and Weber A.** *Z. Phys. Chem., 1926,* **119**
6. **Frakas L.** *Z. Physik. Chem., 1927,* **A125**
7. **Becker R. and Doering W.** Kinetic treatment of nucleation in supersaturated steam. *Annalen der Physik, 1935,* **5F**, *24*
8. **Frenkel J.** Kinetic theory of liquids. *Oxford University Press, London 1946*
9. **Zeldovich J.** *J. Exp. Theor. Phys. (USSR), 1942,* **12**, *525*
10. **McDonald J. E.** Homogeneous nucleation of vapour condensation. *Am. J. Phys., 1962–63,* **30**, *870 and* **31**, *31*
11. **Dunning W. J.** General and theoretical introduction *in 'Nucleation', (ed Zettlemoyer) Marcel Dekker, NY 1969*
12. **Gyarmathy G. and Meyer H.** Spontaneous condensation phenomena. *VDI Forschungsheft, VDI-Verlag 1965,* **508**, *GEGB translation No. 4160*
13. **Bakhtar F. and Piran M.** Thermodynamic properties of supercooled steam. *Int. J. Heat and Fluid Flow, 1979 1(2), 53–62*
14. **Bakhtar F., Ryley D. J., Tubman K. A. and Young J. B.** Nucleation studies in flowing high pressure steam. *Proc. Inst. Mech. Engrs., 1975,* **189** *(41/75)*
15. **Courtney W. G.** Remarks on homogeneous nucleation. *J. Chem. Phys., 1961,* **35**, *2249*
16. **Kantrowitz A.** Nucleation in very rapid vapour expansions. *J. Chem. Phys. 1951,* **19**, *1097*
17. **Young J. B. and Bakhtar F.** A comparison between theoretical calculations and experimental measurements of droplet sizes in nucleating steam flows. *Prace Inst. Maszyn Przeplywowych 1976, 70–72, 259*
18. **Bakhtar F., Ghoneim Z. and Young J. B.** A study of nucleating and wet steam flows in turbines. *Proc. Inst. Mech. Engrs., 1976,* **190**(*44/76*), *545–559*
19. **Bakhtar F. and Heaton A. V.** A theoretical comparative study of wetness problems in a model and full scale turbine. *'Aerothermodynamics of steam turbines' presented at Winter Annual Meeting, ASME, Washington DC 1981*